

Randomness versus deterministic chaos: Effect on invasion percolation clusters

Chung-Kang Peng and Sona Prakash

Center for Polymer Studies and Department of Physics, Boston University, Boston, Massachusetts 02215

Hans J. Herrmann

Service de Physique Theorique, Centre d'Etudes Nucléaires de Saclay, 91191 Gif-sur-Yvette, France

H. Eugene Stanley

Center for Polymer Studies and Department of Physics, Boston University, Boston, Massachusetts 02215

(Received 18 April 1990)

What is the difference between *randomness* and *chaos*? Although one can define randomness and one can define chaos, one cannot easily assess the difference in a practical situation. Here we compare the results of these two antipodal approaches on a specific example. Specifically, we study how well the logistic map in its chaotic regime can be used as quasirandom number generator by calculating pertinent properties of a well-known random process: invasion percolation. Only if $\lambda > \lambda_1^*$ (the first reverse bifurcation point) is a smooth extrapolation in system size possible, and percolation exponents are retrieved. If $\lambda \neq 1$, a sequential filling of the lattice with the random numbers generates a measurable anisotropy in the growth sequence of the clusters, due to short-range correlations.

I. INTRODUCTION

Randomness is an abstract concept that has been very useful but that, strictly speaking, cannot be realized on a computer. Indeed, many models in physics—such as random walks, localization, and percolation—are based on the concept of randomness. The production of random (or “quasirandom”) numbers on a computer is a rather heuristic subject. Based on experience, deterministic algorithms are used which are highly nonlinear and which must pass a certain number of tests.¹

Chaos in deterministic nonlinear maps is one of the major discoveries of the last few decades. Chaos in this sense is also a well-defined concept of great importance in areas like hydrodynamics and pattern formation. *A priori*, chaos has nothing to do with the generation of quasirandom numbers on a computer and is certainly antagonistic to pure randomness because it is deterministic.

The question we raise is to what degree can chaotic sequences be used as quasirandom numbers² and to what extent do the two differ in terms of the properties of a specific model, in our case percolation. Chaotic sequence have been discussed before in the context of the diffusion problem,^{3–6} but the effect of the percolation problem has not yet been investigated.

We consider the simplest one-parameter chaotic map,^{7,8} given by

$$x_{n+1} = 4\lambda x_n(1 - x_n), \quad (1)$$

also known as the logistic map. As we approach the chaotic regime of the logistic map with $\lambda \rightarrow \lambda_c = 0.892\,486\,418\dots$, the period of the sequence of numbers generated by this map becomes infinite. The question is, to what extent does such a sequence behave ran-

domly? Will such a sequence, if used instead of a sequence of numbers drawn from a random-number generator, give us the same critical exponents in simulating percolation? We will address this and other properties of such a sequence at $\lambda = 1$, the most chaotic point, and also at other values of λ in the chaotic regime. We consider invasion percolation,^{9,10} since in this case one does not need to calculate the percolation threshold, whereas in ordinary percolation, we would first have to locate the position of the threshold that would depend on the distribution of numbers in consideration.

There are two important differences between our problem and the corresponding one obtained by replacing the logistic map by a random-number generator. The first is that the probability distribution of numbers generated by the logistic map is not uniform (see Sec. II). The second is that there is a time correlation (which translates to a spatial correlation in our problem) between successive numbers generated by the logistic map. The effect of this is discussed in Sec. III.

We study invasion percolation without trapping on a two-dimensional square lattice of linear size L . We assign numbers generated by the logistic map in sequence along the y axis to the sites (column by column). To grow a cluster, we start by occupying the site at the center of the system and then occupy the perimeter site which has the smallest number on it at the next time step. We repeat the invasion process until the cluster reaches the edges of the vertical (or horizontal) boundaries of the system. We then use the “burning” method proposed in Ref. 11 to study the fractal properties of the cluster and calculate the critical exponents. All the simulations for this work were done on the IBM 3090 computer.

In Sec. IV, we discuss the results of fractal analysis of the infinite cluster obtained for various values of λ . Fi-

nally, in Sec. V, we discuss the growth sequence of the infinite cluster, where we find a marked difference from the random case due to the presence of time correlations, which are discussed in Sec. III.

II. DISTRIBUTION OF NUMBERS

The distribution of numbers generated by the logistic map^{12,13} is not uniform. In the limit of infinitely many numbers, it is of a flattened U shape at $\lambda=1$ [see Fig. 1(a)]. We are interested in seeing whether this property of nonuniformity will affect the fractal analysis of the invasion percolation problem.

At $\lambda=1$, the logistic-map iteration is equivalent to a Bernoulli shift. Consider

$$x_n = \frac{1 - \cos(2\pi\theta_n)}{2}, \quad \text{where } \theta_n \in [0, 1). \quad (2)$$

Substituting this into Eq. (1) with $\lambda=1$, we then obtain the following iteration rule for θ :

$$\theta_{n+1} = 2\theta_n \bmod 1. \quad (3)$$

It is easy to see that the numbers generated by Eq. (3) are

uniformly distributed, provided that they are not in a finite cycle, i.e., if we start with a nonrational seed number θ_0 , then the probability distribution $\tilde{P}(\theta)$ is a constant of order unity. Thus, from (2) the corresponding probability distribution of x is

$$P(x) = \frac{2}{\pi \sin[\cos^{-1}(1-2x)]} = \frac{1}{\pi\sqrt{x(1-x)}}, \quad (4)$$

which looks exactly like Fig. 1(a). The form (4) for $P(x)$ can also be exactly determined from a transformation to the tent map.^{13,14}

We do not expect the nonuniformity of the probability distribution function to affect our results. Since invasion percolation proceeds by a comparison of the values of the random numbers at each time step, one expects that the nonuniform distribution of the individual values of the numbers cannot affect the problem. To see the effect of the nonuniformity of the distribution we draw numbers *randomly* with a probability distribution described by (4), and perform the Monte Carlo simulation of nontrapping invasion percolation for a two-dimensional square lattice. These numbers give correct percolation exponents. Therefore we conclude that the nonuniformity of the distribution does not affect the percolation problem, except in changing the value of p_c . Presuming an absence of correlation between numbers, the value of p_c for the distribution $P(x)$ would be given by

$$\int_0^{p_c} P(x) dx \approx 0.592745, \quad (5)$$

where 0.592745 is the value of p_c obtained in Ref. 15. For $\lambda=1$, this gives $p_c \approx 0.64363$. From simulations we obtain $p_c = 0.65 \pm 0.01$, so the two values are in good agreement with each other.

For $\lambda < 1$, however, the probability distribution cannot be described by a continuous function in the domain $[0, 1]$ [see Fig. 1(b), $\lambda=0.93$]. As we decrease λ within the chaotic regime, we see a qualitative difference in the probability distribution of numbers generated above and below $\lambda = \lambda_1^* \approx 0.91964$, the first reverse bifurcation point.⁸ A gap is found to open up in the distribution at this value of $\lambda = \lambda_1^*$ and the width of this gap increases [Fig. 1(c)] as we decrease λ further. The appearance of this gap plays a crucial role in our problem, as it greatly affects the time correlation of successive numbers generated (Sec. III). In addition, there are also other such gaps in the distribution for values of λ between λ_1^* and 1.0 [for example, the window of period 3 that appears at $\lambda = (1 + \sqrt{8})/4$ and has been treated in Ref. 16], which affect our problem in the same manner.

III. TIME CORRELATIONS

There is clearly a time correlation between numbers generated by the logistic map. However, if these correlations are "short range" we would not expect them to affect the results. In the periodic regime obviously we expect "infinite-range" correlations. The percolation test will verify the nature of the correlations in the chaotic regime.

We find that for $\lambda < \lambda_1^*$, due to the presence of the gap,

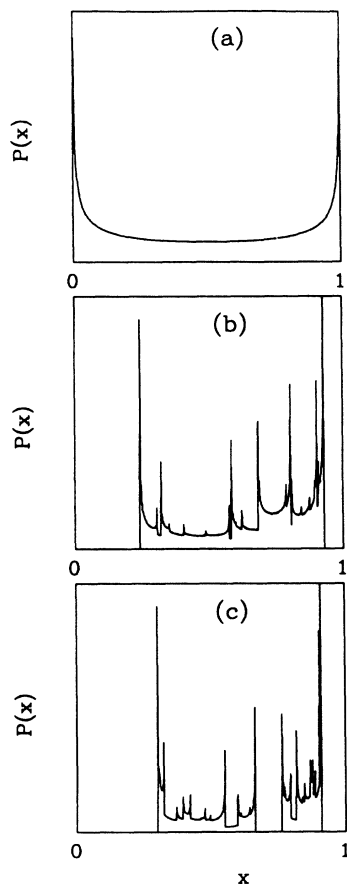


FIG. 1. Probability distribution of numbers generated by the logistic map (10^8 numbers used). (a) $\lambda=1.0$: $P(x)$ is a smooth continuous function given by (4). (b) $\lambda=0.93$: $P(x)$ is discontinuous. (c) $\lambda=0.91$: note the appearance of the gap.

the time sequence of numbers is strongly correlated: it alternates between either side of the gap (high and low) giving rise to effectively infinite-range correlations on the lattice. Since we are placing numbers generated by the logistic map along the y axis in sequence, we have an alternating pattern along the y direction.

For $\lambda > \lambda_1^*$ this alternating pattern continues to exist, but has now a finite correlation length which decreases as we increase λ . In other words, a small (large) number is more probably followed by a large (small) number along the y direction. This tendency greatly affects the sequence of growth of the cluster, which is discussed in Sec. V.

There also exist values of $\lambda > \lambda_1^*$ that have gaps in their probability distribution, e.g., the gap that appears at $\lambda = (1 + \sqrt{8})/4$ has a time sequence of period 3 (Ref. 16) and thus infinite-range correlations exist. However, for $\lambda_1^* < \lambda < 1.0$, as long as we avoid values of λ that are characterized by gaps in the probability distribution, the time correlations do not affect the critical exponents of percolation, as we shall see in Sec. IV. But the time correlations do affect the growth sequence of the cluster, and this is discussed in Sec. V.

We also studied the behavior of the autocorrelation function given by

$$C(m) = \langle X_i X_{i+m} \rangle - \langle X_i \rangle^2, \quad (6)$$

where $\langle \rangle$ is an average over all i with $i = 1, 2, \dots, N$. Between λ_c and λ_1^* , as we increase λ (for fixed N) the fluctuation in $C(m)$ values with m increases [in the periodic regime we expect very little fluctuation since we have a string of numbers in the n cycle and the correlation $C(m)$ should not vary too much with m as long as $m > n$]. Note that $C(m)$ measures the correlation between the numbers placed on two sites that are separated by m steps and therefore that would be neighbors along the x direction for a lattice size of $L = m$. We expect that this might be related to the tendency of directional growth observed for even lattice size; therefore we take only even m . We enclose plots of $C(m)$ versus m for values of λ near λ_1^* . We find that $C(m)$ decays with m , with the range of this decreasing as we increase λ [see Figs. 2(a) and 2(b)]. Note that the range has become very small already at $\lambda = 0.93$, and for higher values of λ this range goes to zero and $C(m)$ is approximately constant with respect to m . Therefore, for lattice sizes $L > L^*$, where L^* is the range of decay of $C(m)$, the effective correlation along the x direction would be the same as the infinite-size case.

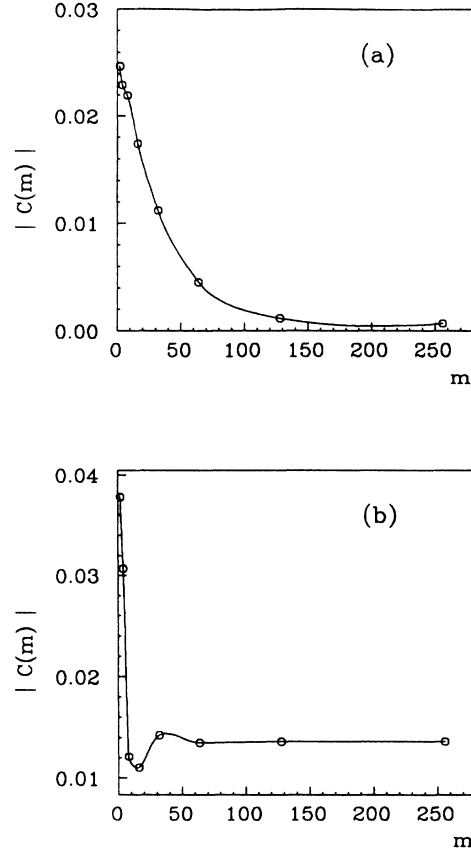


FIG. 2. Decay of autocorrelation function (10^5 numbers used). (a) $\lambda = 0.92$, (b) $\lambda = 0.93$.

IV. PERCOLATION EXPONENTS

We calculated the values of important percolation exponents at the most chaotic point $\lambda = 1.0$ [Figs. 3(a) and 3(b)] as well as at other lower values of λ (Figs. 4 and 5) above the value $\lambda = \lambda_1^*$ for reasons mentioned in Sec. III. We used the burning algorithm of Herrmann, Hong, and Stanley¹¹ and also their conventions for choosing the backbone. The values of the exponents obtained shown in Table I correspond to the following quantities:¹⁷ the mass of the infinite cluster (d_f), the mass of the backbone (d_{BB}), the minimum¹⁸ path (d_{min}), and the number of red^{19,20} bonds (d_{red}). The log-log plots gave asymptotic straight-line behavior and extrapolation to infinite lattice sizes gave correct percolation exponents (Figs. 3 and 4).

TABLE I. Comparison of our calculated percolation exponents and known values.

	d_f	d_{BB}	d_{min}	d_{red}
Known value	$\frac{91}{48}$	1.60 ± 0.05^a	1.13 ± 0.002^b	$\frac{3}{4}^c$
$\lambda = 1.0$	1.86 ± 0.05	1.64 ± 0.05	1.10 ± 0.05	0.74 ± 0.05
$\lambda = 0.93$	1.87 ± 0.05	1.66 ± 0.05	1.12 ± 0.05	0.82 ± 0.05
$\lambda = 0.92$	1.83 ± 0.05	1.64 ± 0.05	1.13 ± 0.05	0.82 ± 0.05

^aReference 11.

^bReference 18.

^cReference 19.

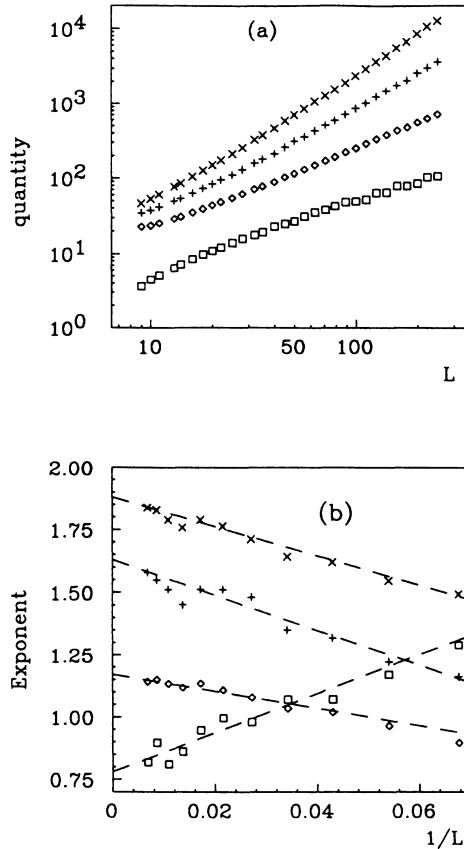


FIG. 3. Percolation exponents obtained using numbers generated by the logistic map $x_{n+1} = 4\lambda x_n(1-x_n)$ at the most chaotic point $\lambda = 1.0$ ($p_c = 0.65 \pm 0.01$). The number of samples averaged over varied from 500 for the largest lattice to 30 000 for the smallest. About 24 h of CPU time were used to generate the data for (a) and (b). (a) Log-log plot of various quantities vs L (linear size). \times , mass of the infinite cluster; $+$, mass of the backbone; \diamond , minimum path; \square , number of red bonds. (b) Exponents by extrapolation.

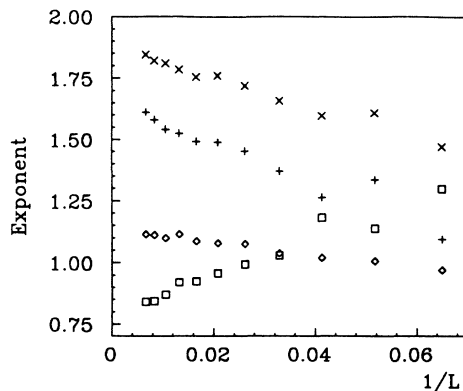


FIG. 4. Exponents by extrapolation for $\lambda = 0.93$. \times , mass of the infinite cluster; $+$, mass of the backbone; \diamond , minimum path; \square , number of red bonds.

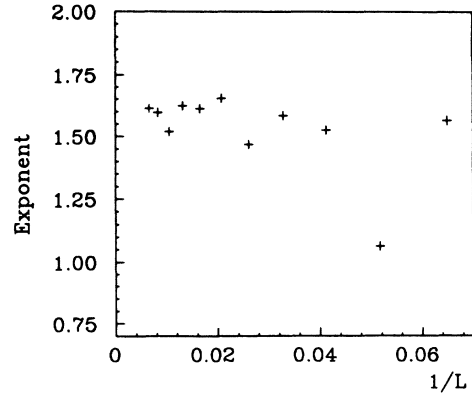


FIG. 5. Extrapolation curve for exponent of the mass of the backbone for $\lambda = 0.92$, near the transition point λ_1^* .

As we approached $\lambda = \lambda_1^*$, the point of transition into a “nonrandom” regime, from above (Fig. 5, with $\lambda = 0.92$), the plots were characterized by large fluctuations but still gave correct asymptotic values of the exponents (Table I). As we cross and go below $\lambda = \lambda_1^*$, however, we enter a regime where the cluster is effectively one dimensional, for reasons that will be explained in detail in Sec. V.

Thus, from the evidence presented in Figs. 3–5, we conclude that the presence of time correlations does not affect the *static* properties of the percolation cluster, as long as we avoid values of λ that have gaps in their probability distribution. However, it does affect the *dynamic* properties, as we shall see in Sec. V.

V. TIME SEQUENCE OF GROWTH OF THE INFINITE CLUSTER

As we watch the invasion percolation cluster grow, we observe some interesting phenomena. Below λ_1^* the cluster is effectively one dimensional. This is because for even-sized lattices, neighbors along the x direction belong on the same side of the gap in the probability distribution mentioned in Secs. II and III. Therefore, once the cluster grows to a site that belongs to a row of small numbers, it continues to grow along the x direction.

For $\lambda > \lambda_1^*$, due to the finite correlation length along the y direction mentioned in Sec. III, the effective correlation along x disappears for large L . However, there is still a tendency to grow continuously along x due to the finite-range correlation along y . In other words, an invaded site with a small number has a high probability of being surrounded along the y direction by sites with large numbers and therefore prefers to grow along x . This tendency of preferential growth along x tends to get weaker with increasing λ and disappears as $\lambda \rightarrow 1$. However, this difference in behavior from the random case that exists even for $\lambda > \lambda_1^*$ does not affect the values of the exponents, as we concluded in Sec. IV. In other words, the structure of the final cluster cannot be distinguished from one grown with random numbers, but the pattern of invasion is quite different, as mentioned above. As we follow the growth of the cluster we can divide the possibili-

ties at each step into three categories.

(a) The next occupied site is the neighbor along the x direction of the most recently occupied one.

(b) The next occupied site is the neighbor along the y direction of the most recently occupied one.

(c) The next occupied site is not a neighbor of the most recently occupied one.

Since this result of the growth sequence of the cluster for $\lambda > \lambda_1^*$ is the only distinguishing factor between such a cluster and one grown by using a random-number generator, we are interested in defining a parameter that describes this difference with the random case, as a function of λ . For this purpose, we define the following quantities.

(i) N_x : The number of sites that are occupied by invasion to the nearest neighbor of the most recently occupied site along the x direction.

(ii) N_y : The number of sites that are occupied by invasion to the nearest neighbor of the most recently occupied site along the y direction.

We first consider the size dependence of the quantity $R = N_x / (N_x + N_y)$ for fixed $\lambda = 0.92, 0.98$ [Figs. 6(a) and 6(b)]. We see that there is a variation, but R saturates to a constant value above some value of L , beyond which

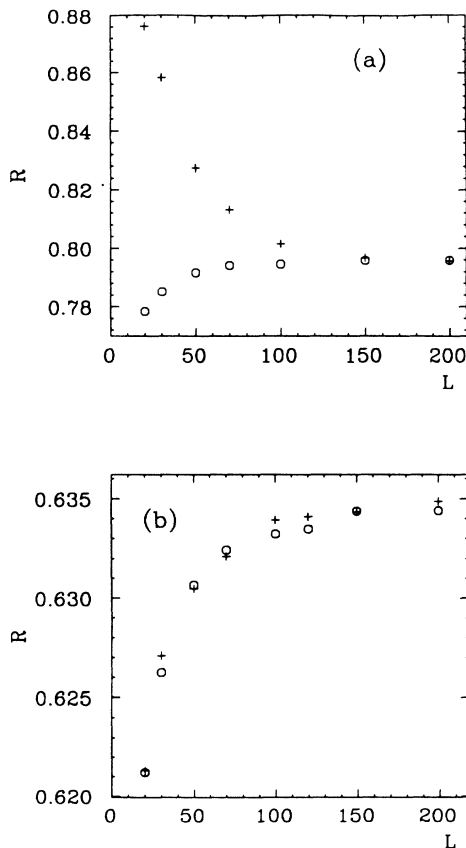


FIG. 6. Dependence of $R = N_x / (N_x + N_y)$ on the lattice size. The numbers of samples averaged over varied from 500 for the largest lattice size used to 10 000 for the smallest. (a) $\lambda = 0.92$: +, correlated column model; o, independent column model. (b) $\lambda = 0.98$: +, correlated column model; o, independent column model.

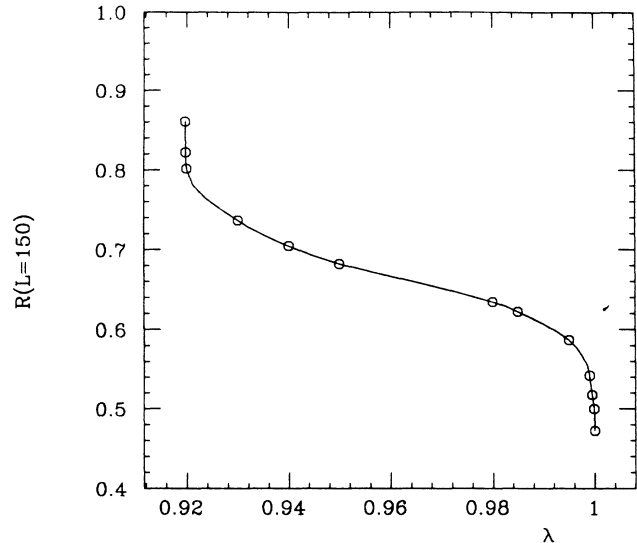


FIG. 7. Dependence of R on λ for $L = 150$, which is effectively the same as the limiting curve $L \rightarrow \infty$. The number of samples averaged over was 500.

finite-size corrections become unimportant. In Fig. 7 we plot R versus λ for a lattice size above the saturation value. Note that R should have the value $\frac{1}{2}$ for the random case and tends towards it as $\lambda \rightarrow 1$. We find that the curve of $R(\lambda)$ has a smooth, well-defined behavior for any L and tends to approach the limiting form that we have plotted in Fig. 7, as $L \rightarrow \infty$. (From Fig. 6 one can see that at $L = 150$, R has already saturated to its infinite-size limit.)

As we inferred in Sec. III, for lattice sizes $L > L^*$, where L^* is the range of decay of the autocorrelation function, the effective correlation along x would be the same as the infinite-size case. And for this model, the infinite-size behavior would be identical to the behavior on a lattice of the corresponding size constructed by putting down numbers from the logistic map on each column independently. In other words, every time we get to a new column, we would choose a new random seed for the logistic map and start iterating again. This would eliminate correlation along x due to finite lattice size. We compared the values of R for different lattice sizes for our “correlated column model” with $\lambda = 0.92$ and 0.98 with the corresponding “independent column model” [see Figs. 6(a) and 6(b)]. For $\lambda = 0.92$, we find that the curves for the two different models [Fig. 6(a)] merge at $L^* \approx 150$, which agrees well with the value of L^* from Fig. 2(a). Also, for $\lambda = 0.98$, the two curves coincide for all values of L , which again agrees with our argument above, since L^* for $\lambda = 0.98$ is almost zero.

VI. SUMMARY AND COMMENTS

We have pointed out in Sec. I that there are two main features that distinguish this problem from the corresponding random one. These are (a) the nonuniformity of the probability distribution, and (b) the existence of correlations between numbers successively generated by the map. In Sec. II, we have treated (a) and come to the

conclusion that it should not in any way affect the properties of the percolation problem, except in changing p_c , the percolation threshold. In Sec. III we have treated (b) and in Sec. IV we have concluded from our results that neither (a) nor (b) affects the static properties of the percolation cluster. In Sec. V we find that (b) does affect the dynamic (growth-pattern-related) properties and we have analyzed this effect. In the following paragraphs, we comment on some related aspects of the problem.

We have verified that the period of the numbers generated by the map is not infinite, even at $\lambda=1$, due to computer truncation. In general, truncation seems to affect the problem in the sense that there is no “truly infinite” period in the chaotic regime. For example, at $\lambda=1$ there are two periods of length 160 853 385 and 105 364 478, respectively, when we use double-precision numbers. However, from studying correlations above [fluctuation in $C(m)$ with m for $\lambda=1$ has disappeared at $N=10^6$], it seems that there is still an “effective period” less than 10^6 , i.e., there is repetitive fine structure within a period. Thus it seems that the larger system sizes will be influenced more by this “effective period” and therefore data at large L may not be reliable. This would explain the erratic behavior that we found above $L \simeq 250$ and therefore we did the extrapolation on the basis of results obtained for lattice sizes below this value (Figs. 3–5). It is well known that good quasi-random-number generators also have this problem, in that their maximal period is many orders of magnitude longer than their effective period. As an example for a large-scale computation in which such a problem arises, one can cite Normand,

Herrmann, and Hajjar.²¹

Of course, another reason for the aforementioned erratic behavior is simply that we might not have had enough statistics. In particular, the fluctuation in the number of red bonds does not show a tendency to decrease as we increase the lattice size. We found that the running average seems to stabilize around 4000 runs for $L=10$, but for $L=160$, it still is not stabilized around 4000 runs, whereas one would expect it to do so much earlier. This behavior can also be seen from the large fluctuations in the exponent for the number of red bonds even at $\lambda=1$ [in Fig. 3(b)].

It would be interesting to use invasion percolation with the logistic map as the number generator as a model of some special kind of porous medium which exhibits the kind of correlation discussed in Secs. III and V, along one direction; namely, that the resistance to flow of the medium has a tendency to alternate between large and small values, within some finite correlation length.

ACKNOWLEDGMENTS

We are grateful for discussions with P. Alström, A. Bunde, A. Coniglio, C. Godreche, S. Havlin, M. Nauenberg, R. Selinger, F. Sciortino, S. Sastry, D. Stassinopoulos, and especially with G. Huber, and for support from North Atlantic Treaty Organization, Office of Naval Research, National Science Foundation, and the Boston University Academic Computing Center.

¹D. E. Knuth, *Seminumerical Algorithm* (Addison-Wesley, Reading, MA, 1981), Chap. 3.

²S. Ulam and J. von Neumann, *von Neumann's Collected Works* (Pergamon, New York, 1961), Chap. 5, p. 768.

³T. Geisel and J. Nierwetberg, *Phys. Rev. Lett.* **48**, 7 (1982).

⁴S. Grossmann and H. Fujisaka, *Phys. Rev. A* **26**, 504 (1982).

⁵C. Beck and G. Roepstorff, *Physica A* **145**, 1 (1987).

⁶T. Shimizu, *Physica A* **164**, 123 (1990).

⁷M. Feigenbaum, *Los Alamos Sci.* **1**, 4 (1980).

⁸S. Grossmann and S. Thomae, *Z. Naturforsch.* **32A**, 1353 (1977).

⁹R. Chandler, J. Koplik, K. Lerman, and J. F. Willemsen, *J. Fluid Mech.* **119**, 249 (1982).

¹⁰D. Wilkinson and J. F. Willemsen, *J. Phys. A* **16**, 3365 (1983).

¹¹H. J. Herrmann, D. C. Hong, and H. E. Stanley, *J. Phys. A* **17**, L261 (1984).

¹²R. Shaw, *Z. Naturforsch.* **36A**, 80 (1981).

¹³A. J. Lichtenberg and M. A. Lieberman, *Regular and Stochastic Motion* (Springer-Verlag, Berlin, 1983).

¹⁴H. G. Schuster, *Deterministic Chaos* (Physik-Verlag, Weinheim, 1984).

¹⁵R. M. Ziff and B. Sapoval, *J. Phys. A* **19**, L1169 (1986).

¹⁶J. E. Hirsch, B. A. Huberman, and D. J. Scalapino, *Phys. Rev. A* **25**, 519 (1982).

¹⁷D. Stauffer, *Introduction to Percolation Theory* (Taylor and Francis, Philadelphia, 1985).

¹⁸H. J. Herrmann and H. E. Stanley, *J. Phys. A* **21**, L829 (1988).

¹⁹H. E. Stanley, *J. Phys. A* **10**, L211 (1977).

²⁰A. Coniglio, *Phys. Rev. Lett.* **46**, 250 (1980); see also A. Coniglio, in *Correlations and Connectivity: Geometric Aspects of Physics, Chemistry, and Biology*, edited by H. E. Stanley and N. Ostrowsky (Kluwer Academic, Dordrecht, 1990).

²¹J. M. Normand, H. J. Herrmann, and M. Hajjar, *J. Stat. Phys.* **52**, 441 (1988).